Received: 11 July 2022 | Revised: 25 May 2023 | Accepted: 31 May 2023

DOI: 10.1111/pce.14644

ORIGINAL ARTICLE

Plant, Cell & Environment | WILEY

ZmEREB57 regulates OPDA synthesis and enhances salt stress tolerance through two distinct signalling pathways in *Zea mays*

Jiantang Zhu[1] | Xuening Wei[1] | Chaoshu Yin[1] | Hui Zhou[1] | Jiahui Yan[1] | Wenxing He[1] | Jianbing Yan[2] | Hui Li[1]

[1]School of Biological Science and Technology, University of Jinan, Jinan, China

[2]National Key Laboratory of Crop Genetic Improvement, Huazhong Agricultural University, Wuhan, China

Correspondence
Hui Li, School of Biological Science and Technology, University of Jinan, Jinan 250022, China.
Email: bio_lih@ujn.edu.cn

Funding information
National Natural Science Foundation of China, Grant/Award Numbers: 31901497, 32272075; National Key Research and Development Program of China, Grant/Award Number: 2022YFD1201502; Science and Technology Program of University of Jinan, Grant/Award Number: XKY2207

Abstract

In plant, APETALA2/ethylene-responsive factor (AP2/ERF)-domain transcription factors are important in regulating abiotic stress tolerance. In this study, *ZmEREB57* encoding a AP2/ERF transcription factor was identified and its function was investigated in maize. ZmEREB57 is a nuclear protein with transactivation activity induced by several abiotic stress types. Furthermore, two CRISPR/Cas9 knockout lines of *ZmEREB57* showed enhanced sensitivity to saline conditions, whereas the overexpression of *ZmEREB57* increased salt tolerance in maize and Arabidopsis. DNA affinity purification sequencing (DAP-Seq) analysis revealed that ZmEREB57 notably regulates target genes by binding to promoters containing an O-box-like motif (CCGGCC). ZmEREB57 directly binds to the promoter of *ZmAOC2* involved in the synthesis of 12-oxo-phytodienoic acid (OPDA) and jasmonic acid (JA). Transcriptome analysis revealed that several genes involved in regulating stress and redox homeostasis showed differential expression patterns in OPDA- and JA-treated maize seedlings exposed to salt stress compared to those treated with salt stress alone. Analysis of mutants deficient in the biosynthesis of OPDA and JA revealed that OPDA functions as a signalling molecule in the salt response. Our results indicate that ZmEREB57 involves in salt tolerance by regulating OPDA and JA signalling and confirm early observations that OPDA signalling functions independently of JA signalling.

KEYWORDS
AP2/ERF-domain transcription factor 57, JA-independent, maize, OPDA/JA synthesis, salt stress

1 | INTRODUCTION

Abiotic stresses, such as high salinity, drought, and extreme temperatures, can adversely affect the growth and productivity of plants, particularly of crops. Thus, plants have developed diverse mechanisms to cope with the inhibitory effects of environmental conditions (Bartels & Sunkar, 2005). Jasmonates (JAs) are lipid-derived signal transducer molecules that play important roles in plant development and that mediate responses to abiotic stress (Wasternack & Hause, 2013). JAs accumulate in response to drought and high salinity, leading to the expression of stress-response genes (Jung et al., 2007). In rice, the endogenous JA content in a salt-tolerant cultivar was higher than that in a salt-sensitive cultivar (Kang et al., 2005), and JA biosynthesis was strongly induced by drought stress (Takeuchi et al., 2011).

The oxylipin 12-oxo-phytodienoic acid (OPDA) is an essential precursor of JA, which is synthesised via the α-linolenic acid (ALA)

metabolic pathway (Chini et al., 2018). Lipases aid in the release of ALA from plastidial membrane lipids. ALA is then oxygenated using 13-lipoxygenases (LOX) to form 13-hydroperoxylinolenic acid (Wasternack & Hause, 2013), which is then converted into 12, 13-epoxyoctadecatrienoic acid in chloroplasts by allene oxide synthase (AOS). Next, 12, 13-epoxyoctadecatrienoic acid is used as a substrate by allene oxide cyclase (AOC) to produce OPDA (Dave & Graham, 2012; Wasternack & Strnad, 2016), which is subsequently transported into the peroxisome, where it undergoes reduction by OPDA reductase 3 (OPR3) and β-oxidation to generate JA (Dave & Graham, 2012; Kienow et al., 2008).

The bioactive form of jasmonoyl-L-isoleucine (JA-Ile) mediates the interaction between coronatine-insensitive protein 1 (COI1) and JA-ZIM domain (JAZ) repressors to form the COI1-JAZ co-receptor complex (Staswick & Tiryaki, 2004). Under low-JA conditions, JAZ proteins act as transcriptional repressors of gene expression. In response to elevated JA levels, the JA-Ile-mediated COI1-JAZ interaction triggers the ubiquitination of JAZ repressors and their subsequent degradation by the proteasome, activating several transcription factors (TFs) that regulate specific physiological responses (Thines et al., 2007; Zhang et al., 2017).

Studies have suggested that OPDA is involved in biotic and abiotic stress responses, embryo development, and seed germination (Satoh et al., 2014; Savchenko et al., 2014; Savchenko & Dehesh, 2014). Several studies have shown that OPDA functions in a JA/COI1-independent manner. For example, studies of JA biosynthetic and signalling mutants in Arabidopsis demonstrated that OPDA could also inhibit seed germination together with abscisic acid (ABA), independent of the COI1-dependent signalling pathway (Dave et al., 2011). OPDA, but not JA, is found in *Marchantia polymorpha* and *Physcomitrella patens*, where it has specific functions in defence and development (Stumpe et al., 2010; Yamamoto et al., 2015). In Arabidopsis, many genes responding to various abiotic stresses were shown to be specifically induced by OPDA but not to respond to JAs. While *AtVSP2* (vegetative storage protein 2) is a known jasmonate-responsive gene, *ZAT10* (encoding a salt-tolerance zinc-finger transcription factor), *ERF5*, *DREB2A*, *GST6* and *FAD-OXR* (FAD-linked oxidoreductase) are responsive to OPDA but not JA (Abbaraju et al., 2022; Borkiewicz et al., 2020; Hao et al., 2020; Qin et al., 2007; Taki et al., 2005).

The APETALA2/ethylene-responsive factor (AP2/ERF) superfamily is one of the largest groups of TFs in plants. AP2/ERF TFs contain a highly conserved AP2 DNA-binding domain (approximately 60-amino acids), which binds to the GCC-box (GCCGCC) and/or dehydration-responsive element (DRE)/C-repeat element to directly regulate genes that are essential in plant development, defence against pathogens, and stress responses (Mizoi et al., 2012; Sakuma et al., 2002; Xu et al., 2011). Certain ERF family members respond to phytohormones and abiotic stress signals (Sugano et al., 2013). For example, rice *OsEBP2*, an ERF family member, was induced in response to compatible interactions with the blast fungus and was transiently induced by treatments with MeJA, ABA, and ethylene, indicating the possible role of *OsEBP2* in both biotic and abiotic stresses (Lin et al., 2007). Furthermore, under wounding or drought stress conditions, Arabidopsis octadecanoid-responsive AP2/ERF-domain TF 47 (AtORA47) is involved in the biosynthesis of JA, ABA, ethylene, and salicylic acid by binding to the *cis*-element of the O-box [(NC/GT) CGNCC] (Chen et al., 2016).

Less is known about the synthesis and function of JA in monocot plants such as rice and maize, than in dicots. However, it has been shown that chloroplast-localised ZmLOX8 plays a fundamental role in the accumulation of OPDA and JA, and *ZmAOS* and *ZmAOC* have also been implicated in JA biosynthesis (Acosta et al., 2009; Zhang et al., 2005). In the present study, the maize ethylene-responsive element binding factor 57 (*ZmEREB57*) was isolated and investigated in relation to its response to salt stress. ZmEREB57 was found to positively modulate salt tolerance. In this study, we present evidence that ZmEREB57 binds to the O-box-like element in the promoter of *ZmAOC2*, regulating its expression and, consequently, the biosynthesis of OPDA and JA, which feed into two separate salt stress response signalling pathways.

2 | MATERIALS AND METHODS

2.1 | ZmEREB57 phylogenetic analysis

The *ZmEREB57* full-length complementary DNA (cDNA) was amplified by PCR using the gene-specific primers listed in Table S1. Five sequences, including the full open reading frame of *ZmEREB57* and homologous genes in maize (*Zea mays*), rice (*Oryza sativa*), Arabidopsis (*Arabidopsis thaliana*), *Brachypodium distachyon* and *Glycine Max*, were obtained from NCBI (https://www.ncbi.nlm.nih.gov/). The amino acid sequences encoded by these genes were aligned using ClustalW (2.0) (http://www.clustal.org/). The phylogenetic tree was constructed in MEGA v5.1 (https://megasoftware.net/) using the neighbour-joining method with 1000 bootstrap replicates in the *p*-distance model method.

2.2 | Subcellular localisation and transcription activation assay

The *ZmEREB57* or *ZmAOC2* coding region was cloned into the pBI221-GFP vector using the Gateway LR reaction (Invitrogen; gene-specific primers are listed in Table S1) to produce the *35S:ZmEREB57*-GFP or *35S:ZmAOC2*-GFP construct. An empty *35S*:GFP vector was used as a control. Transient expression of green fluorescent protein (GFP)-fused proteins in maize protoplasts was performed as described by Cao et al. (2014), and transfected cells were observed using a confocal laser scanning microscope (Leica TCS SP2; Leica Microsystems GmbH).

For transcriptional activation analysis, full-length *ZmEREB57* was ligated into *EcoRI* and *BamHI*-digested fragments of the pGBKT7 vector (Clontech) using gene-specific primers (Table S1). The recombinant plasmid pGBKT7-ZmEREB57 was transformed into Y2H Gold yeast cells using pGADT7. The interaction between pGBKT7-53 and

pGADT7-LargeT was used as a positive control, and the empty pGBKT7 vector was used as a negative control. The transformed yeast cells were cultured on SD/-Trp and SD/-Trp/-Leu/-Ade/X-α-Gal plates, respectively. The plates were then incubated for 3 days at 28°C.

2.3 | *ZmEREB57* expression analysis

Seeds of the maize inbred KN5585 line were surface-sterilised and germinated on filter paper for 4 days at 28°C in the dark. Seedlings with a primary root 2-cm in length were transferred to Hoagland's nutrient solution and grown in a greenhouse (14 h/10 h of light/dark) at 32°C in the day and 25°C at night until the plants reached the three-leaf stage. The seedlings were then watered with 20% (wt/vol) PEG6000, 200 mM NaCl, or 1.5 mM H_2O_2 solution. For phytohormone treatment, ABA or JA is first dissolved in 2 mL anhydrous ethanol and then diluted with 5 mL H_2O, eventually, diluted to 0.1 mM or 100 μM with the culture solution, respectively. The treated seedlings were harvested at 0, 3, 6, 9, 12 and 24 h, frozen immediately in liquid nitrogen, and stored at −80°C. Total RNA was extracted using the TRIzol reagent (Tiangen) according to the manufacturer's instructions. cDNA was synthesised using M-MLV reverse transcriptase (Takara Bio, Inc.) according to the manufacturer's protocol. Quantitative (q)PCR was performed on a Bio-Rad CFX96 using the SsoFast EvaGreen Supermix (Bio-Rad), and a maize tube (NP_0011054557) was used as an internal control. Primer sequences used in this study are listed in Table S1.

2.4 | Generation and analysis of maize mutant lines

Knockout *zmereb57* mutant lines were generated from the KN5585 inbred line using the CRISPR-Cas9 system (Xing et al., 2014). Briefly, a pCAMBIA-derived CRISPR-Cas9 binary vector with two guide RNA (gRNA) expression cassettes targeting two adjacent sites of *ZmEREB57* was generated, transformed into *Agrobacterium* EHA105 strain, and subsequently transformed into immature embryos of KN5585 inbred lines. To identify positive CRISPR-Cas9 knockout lines, PCR amplicons encompassing the gRNA-targeted sites for each transgenic plant were sequenced using Sanger sequencing. The primers used for gene editing and plasmid construction are listed in Table S1.

The *ZmAOC2* and *ZmOPR3* alleles were isolated from the UniformMu population, where the Mu-active lines were introgressed into inbred B73 genetic background (Liang et al., 2019). The PCR was based on primers targeting *ZmAOC2* or *ZmOPR3* and Mu (gene-specific primers are listed in Table S1).

2.5 | Generation of transgenic *ZmEREB57* overexpression lines in maize or Arabidopsis

To generate transgenic plants, full-length *ZmEREB57* was inserted into the pCAMBIA3301 vector with a GFP/HA-tag driven by the maize ubiquitin promoter using the Gateway LR reaction (Invitrogen; gene-specific primers are listed in Table S1). The recombinant vectors were then integrated into the KN5585 maize inbred line (wild-type [WT]) via embryo-derived callus transformation (Jia et al., 2020) using the *Agrobacterium tumefaciens* strain EHA105 (Wemibio Co., Changzhou, China). Positive transgenic plants from each generation were identified using specific PCR analysis. *ZmEREB57* expression in transgenic plants was determined using qRT-PCR and western blotting. Homozygous overexpression lines were obtained by antiherbicide selection of self-pollinated T_1 and T_2 plants. Two independent homozygous T_2 lines (OE1 and OE2) were selected for subsequent experiments.

The CDS of *ZmEREB57* was inserted into the pcambia1300 vector (Invitrogen; gene-specific primers are listed in Table S1), and then the recombinant constructs were transformed into *A. thaliana* wild type using the floral dip method with *A. tumefaciens* strain GV3101 (Clough & Bent, 1998). The aerial parts of healthy Arabidopsis plants were gently submerged for 1–3 min in a small beaker containing a suspension of Agrobacterium cells. The treated plants were kept in the dark for 24 h and then moved back to the growth chamber or the greenhouse. Antibiotic-resistant plants were selected by screening successive generations using kanamycin (50 mg/L). Three overexpression lines (At-OE1, At-OE2 and At-OE3) were selected for phenotypic analysis. An *At1g74930* mutant (*atora47*: SALK_084382), the wild-type allele encoding a *ZmEREB57* homolog in *A. thaliana*, was obtained from TAIR (www.arabidopsis.org). To verify whether *ZmEREB57* was responsible for the *atora47* mutant phenotype, full-length *ZmEREB57* was transformed into the *atora47* mutant to obtain a restorer line ($atora47^{Com\text{-}ZmEREB57}$).

2.6 | Phenotypic response of transgenic and non-transgenic maize or Arabidopsis lines to salt stress

To evaluate salt stress tolerance, seeds of the WT and T3 transgenic lines were grown to the three-leaf stage in soil for 2 weeks, and then the seedlings were irrigated with 200 mM NaCl solution daily for 8 days. For the phytohormone treatments, maize seedlings at the three-leaf stage were treated using Hoagland's solution containing either 200 mM NaCl or 200 mM NaCl + 100 μM OPDA or 200 mM NaCl + 100 μM JA for 4 days. Each experiment was performed in triplicate. Transgenic and non-transgenic Arabidopsis seeds were grown in soil under normal conditions for 4 weeks and were then adequately irrigated with a NaCl solution (200 mM) every day for 8 days. The leaf water potential and chlorophyll content were examined as previously described (Ni et al., 2019). Each experiment was performed in triplicate.

2.7 | DAP-seq assay

DNA affinity purification sequencing (DAP-seq) and data analysis were conducted as previously described, with minor modifications

(Bartlett et al., 2017). Genomic DNA (gDNA) was extracted from young maize leaf tissues. A gDNA DAP-seq library was prepared by attaching a short DNA sequencing adaptor to purified and fragmented gDNA. The adapter sequences were truncated Illumina TruSeq adapters; the TruSeq Universal and index adapters corresponded to the DAP-Seq Adapter A and Adapter B. The DAP-seq gDNA library was prepared using KAPA HiFi HotStart ReadyMix with unique index primers. *ZmEREB57* was fused to HaloTag using the pFN19K HaloTag T7 SP6 Flexi Vector kit (cat. no. G184A) (Promega). ZmEREB57 fused to HaloTag was expressed using the TnT SP6 High-Yield Germ Protein Expression System (L3260) (Promega) and purified using Magne HaloTag Beads (G7281) (Promega). The Magne HaloTag Beads and ZmEREB57-HaloTag mixture were incubated with 500 ng DNA library in 40 µL PBS (phosphate buffered saline) buffer with slow rotation in a cold room for 1.5 h. The beads were washed five times with 200 µL PBS + NP40 (0.005%), resuspended in PBS buffer, the supernatant was removed, 25 µL EB buffer was added, and samples were incubated for 10 min at 98°C to elute the bound DNA from the beads. The DAP-seq library concentration was corrected based on the library fragment size to achieve a specific read count. As described above, negative-control mock DAP-seq libraries were prepared without adding proteins to the beads. The final products were selected from 250 to 500 bp for ChIP-seq sequencing.

Target genes were defined as those containing DAP-seq peaks located within the transcribed regions of genes, introns, 2 kb upstream of the transcription start site (TSS), or 2 kb downstream from the transcription termination site (TTS). DAP-seq reads were aligned to the maize genome using Bowtie 2.2.3 with the default parameters (Langmead & Salzberg, 2012). DAP-seq peaks were identified by MACS2 (version 2.0.10) with default parameters and a *q* value <0.05 (Zhang et al., 2008). The core motifs were identified using MEME-ChIP (Machanick & Bailey, 2011).

2.8 | Yeast one-hybrid (Y1H) assay

The coding sequence of *ZmEREB57* was obtained, digested with *EcoRI* and *BamHI*, and inserted into the pGADT7-AD vector (Clontech) containing the GAL4 active domain. The promoters of *ZmAOC2* were cloned into the *KpnI* and *XhoI* sites of the pHiS2.1 vector. Plasmids were transformed in pairs into the yeast AH109 strain, which was then selected on SD/-Trp/-Leu and SD/-Trp/-Leu/-His media. The plates were then incubated for 3 days at 28°C. All primers used for the constructs are listed in Table S1.

2.9 | Luciferase assay

Full-length *ZmEREB57* and the promoter fragments of *ZmAOC2* were inserted into the 35S:GFP and pGreenII 0800:LUC vectors, respectively (gene-specific primers are listed in Table S1). The recombinant vectors were transformed into tobacco (*Nicotiana benthamiana*) leaves using the agrobacterial infiltration method (*A. tumefaciens strain* GV3101). The luciferase signal was detected 72 h post-transfection using a Tanon 5200 multi-chemiluminescence imaging system (Tanon Science & Technology Co.).

2.10 | Electrophoretic mobility shift assay (EMSA)

The full-length *ZmEREB57* coding region was cloned into the pET30a vector (gene-specific primers are listed in Table S1). The recombinant fusion plasmid was transformed into the *Escherichia coli* BL21(DE3) strain, and overexpression of the cloned genes was induced with 0.5 mM isopropyl-β-D-thiogalactoside at 37°C for 7 h. For isolation and purification of the recombinant protein, bacterial cells were pelleted after induction, resuspended in 10 mL ice-cold binding buffer (0.5 M NaCl, 20 mM Tris-HCl, 5 mM imidazole, and pH 7.9), and sonicated on ice for 10 min (30 s pulse/min), until the samples were no longer viscous. Following centrifugation at 12 000*g* for 15 min at 4°C, supernatants were collected, loaded onto His-Bind® Resin columns (EMD Millipore; Merck KGaA), and the recombinant ZmEREB57 protein was eluted using elution buffer (0.5 M NaCl, 20 mM Tris-HCl, 1 M imidazole, and pH 7.9). The 5'-end biotin probes were generated using a DIG Gel Shift Kit (Roche, China) (Table S1), and the probes without a biotin label were set as competitor probes. EMSAs for detecting interactions between *ZmEREB57* and *ZmAOC2* promoter were according to the methods of the DIG Gel Shift Kit (Roche).

2.11 | Detection of phytohormones

Phytohormone content was detected using MetWare (http://www.metware.cn/) based on the AB Sciex QTRAP 6500 LC-MS/MS platform. For each replicate, approximately 2 g (fresh weight) of fresh maize samples, including KN5585 and mutants, were harvested at the three-leaf stage after treatment with or without 200 mM NaCl, immediately frozen, homogenised in liquid nitrogen, and stored at −80°C until further use. Each sample was dissolved in 3 mL of 2-propanol/H_2O/concentrated HCl (2:1:0.002, vol/vol/vol) extraction solvent, and H_2JA (TCI AMERICA) was added as an internal standard. The mixture was vortexed for 10 min and centrifuged at 13 000*g* at 4°C for 5 min. The lower phase was then transferred to a clean plastic microtube. The samples were allowed to evaporate to dryness, dissolved in 100 µL 80% methanol (vol/vol), and filtered through a 0.22-µm membrane filter for liquid chromatography-mass spectrometry (LC-MS/MS) analysis. A linear ion trap Orbitrap mass spectrometer (Orbitrap Elite; Thermo Fisher Scientific) coupled online with an UPLC system (ACQUITY UPLC; Waters) was used for quantitation. JA and OPDA were separated using a C18 column (Waters) operated in negative-ion mode. OPDA (Item No. 88520, Cayman Chemical) and JA (Product No. 14631, Sigma-Aldrich) were used as standards. Data were analyzed using three biological replicates.

2.12 | RNA-seq analysis

The KN5585 WT plants were treated with or without 200 mM NaCl or 200 mM NaCl + 100 μM OPDA or 100 μM JA at the three-leaf stage. On day 4 of the treatment, approximately 0.5 g of leaves (fresh weight) were collected and immediately frozen in liquid nitrogen, with three biological replicates taken for each treatment. Total RNA was extracted using TRIzol reagent (TIANGEN BIOTECH). The cDNA library was constructed using the NEBNext Ultra RNA Library Prep Kit for Illumina (NEB), according to the manufacturer's instructions. Cutadapt software (https://cutadapt.readthedocs.io/) was used to exclude reads containing adapter contamination and low-quality and undetermined bases. RNA-seq data were normalised to rounded values of fragments per kilobase million. Differentially expressed messenger RNAs were identified by selecting those with fold-changes >2 or <0.5 and $p < 0.05$, using edgeR (https://bioconductor.org/packages/release/bioc/html/edgeR.html) or DESeq. 2 (https://bioconductor.org/packages/release/bioc/html/DESeq. 2.html) in R (https://www.r-project.org/) (Anders & Huber, 2010), followed by gene ontology (GO) term enrichment analysis (Young et al., 2010).

2.13 | Statistical analysis

Two-way analysis of variance and Tukey's post hoc test were used to compare the measurements and characteristics of the plant genotypes tested in this study. A statistical p value of <0.05 was considered a significant difference.

3 | RESULTS

3.1 | Sequence analysis of ZmEREB57

RNA-seq studies were performed to establish how salt stress (200 mM NaCl) impacted the transcriptome of the inbred maize KN5585 line. In total, 12 146 differentially expressed genes (DEGs), comprised of 5005 upregulated and 7141 downregulated genes were identified (Table S2). Among these DEGs, the gene *Zm00001eb193060*, which encodes ethylene-responsive element binding factor 57 (ZmEREB57) belonging to the AP2/ERF TF family, was significantly upregulated under salt stress (fold change = 3.6356, $p = 0.0002$). To examine the role of this gene under salt stress conditions, the full CDS of *ZmEREB57* was isolated from the maize genome database (https://www.maizegdb.org/). The gene contained an open reading frame of 705 bp encoding 234 amino acids, and the deduced protein sequence included the conserved AP2/ERF domain (Figure S1a). Sequence alignment and phylogenetic analysis of ZmEREB57 and proteins from the AP2/ERF gene family in Arabidopsis, rice, soybean and Brachypodium indicated high similarity among the homologs (Figure S1a,b). Alignment analysis revealed 31.9% amino acid sequence identity between ZmEREB57 and AtORA47 (the octadecanoid-responsive AP2/ERF-domain TF in Arabidopsis), as well as highly similar predicted three-dimensional structures, containing a long C-terminal α-helix and a three-stranded anti-parallel β-sheet (β1–β3) (Figure S1c). These results indicate that ZmEREB57 is a member of the AP2/ERF TFs.

3.2 | ZmEREB57 localises to the nucleus and exhibits transcription activation activity

To determine the subcellular localisation of ZmEREB57, a ZmEREB57-GFP fusion protein expressed under the control of the CaMV *35S* promoter was transformed into maize protoplasts cells. Microscopic images showed that the ZmEREB57-GFP construct induced fluorescence only in the nuclei, whereas the fluorescent signals of the control GFP construct were observed throughout the cell (Figure 1a). These results indicated that ZmEREB57 is localised in the nucleus.

A transactivation assay was performed in yeast to determine whether ZmEREB57 acts as a transcriptional activator (Figure 1b). All yeast cells grew on the SD/-Trp medium (Figure 1b). In contrast, only transformants containing the pBD-ZmEREB57 vector and positive controls could grow on a more stringent medium (SD/-Trp/-His/-Ade plates) and appeared blue in the X-a-gal assay (Figure 1b), indicating that ZmEREB57 could activate transcription in yeast.

3.3 | Expression of *ZmEREB57* can be induced by multiple types of abiotic stress

Quantitative PCR was performed to determine *ZmEREB57* transcript levels in maize plants subjected to dehydration (PEG6000), NaCl, H_2O_2, ABA and JA treatments (Figure S2). The results showed that *ZmEREB57* was strikingly induced under these five treatments. In particular, the expression level of *ZmEREB57* peaked after 12 h of salt or JA treatment and was induced by more than 50- or 20-fold, respectively, compared with that under normal conditions (Figure S2). In response to drought and oxidative stress, a sharp increase in *ZmEREB57* transcription was observed 3 h after treatment, with a peak at 12 h (Figure S2). ABA treatment resulted in similar effects, with transcription remaining higher than the baseline, even 24 h after phytohormone treatment (Figure S2).

3.4 | *ZmEREB57* enhances salt tolerance in maize plants

Considering that *ZmEREB57* expression was significantly upregulated under salt stress, we generated a series of maize genetic materials, including two *ZmEREB57*-overexpressing lines (OE1 and OE2) and two independent mutant lines using the CRISPR-Cas9 system, $ZmEREB57^{crispr}$–1 (*zmereb57-1*) and $ZmEREB57^{crispr}$–2 (*zmereb57-2*), to verify the biological function of *ZmEREB57*. In *zmereb57-1* and *zmereb57-2*, respectively, a 2- and 4-bp deletion, caused frameshifting

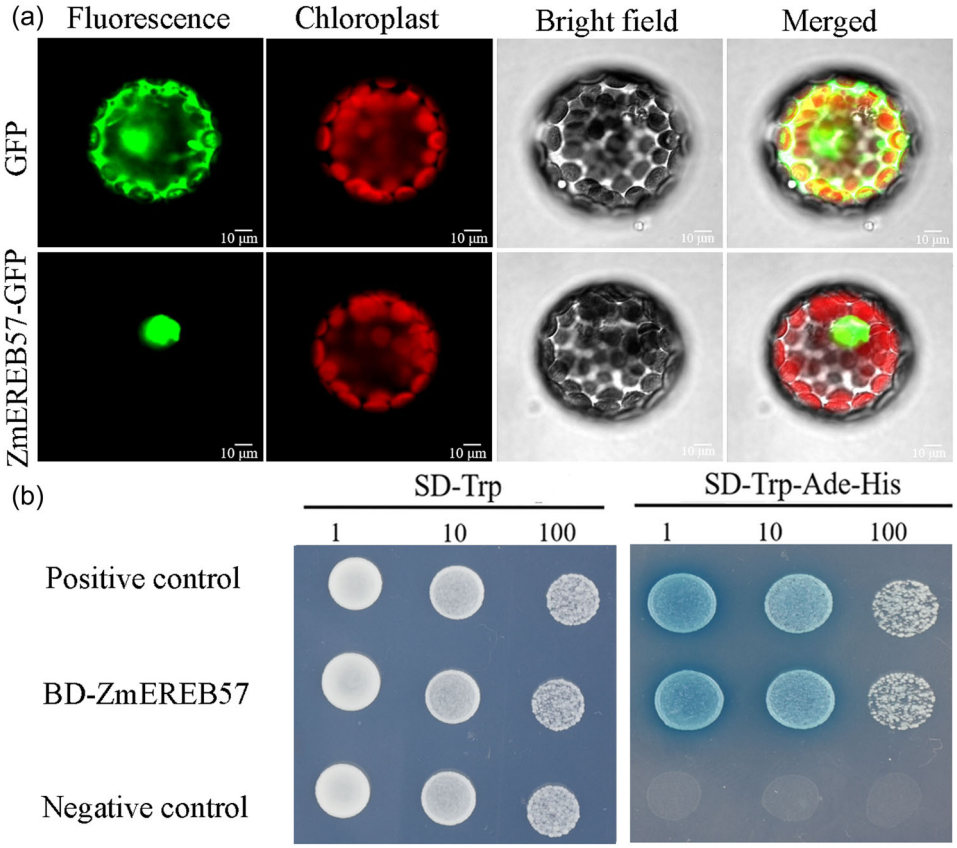

FIGURE 1 ZmEREB57 subcellular localisation and transactivation activity assays. (a) The subcellular localisation of ZmEREB57-GFP in maize protoplasts cells was visualised using confocal laser scanning microscopy. Scale bar = 10 μm. (b) Transactivation assay of ZmEREB57. The construct of pGBKT7-ZmEREB57 was transformed into the yeast Y2H gold strain, which was examined on SD/-Trp and SD/-Trp/-Leu/-Ade/X-α-gal plates. The interaction between pGBKT7-53 and pGADT7-T served as a positive control, and the empty pGBKT7 vector was used as a negative control. GFP, green fluorescent protein; ZmEREB57, *Zea mays* Ethylene Responsive Element Binding Factor 57. [Color figure can be viewed at wileyonlinelibrary.com]

and truncation of the resulting protein, and the abundance of *ZmEREB57* transcript in both mutants was significantly lower than that in WT maize (Figure 2a,b and Figure S3). We used the OE and mutant lines to investigated the effects of altered *ZmEREB57* expression on tolerance to salt stress (Figure 2c). When 2 weeks old hydroponically grown maize plants were treated with 200 mM NaCl for 8 days, the two CRISPR/Cas9 knockout lines exhibited notably enhanced sensitivity to salt stress with enhanced withering and bleaching of leaves compared to the WT, whereas the OE lines displayed markedly less chlorosis than the WT (Figure 2c). Correspondingly, the decrease in the relative water content (RWC) and chlorophyll contents of *zmereb57-1* and *zmereb57-2* was more notable than that in the WT and OE lines (Figure 2d,e). These results demonstrate that *ZmEREB57* is involved in salt stress response in maize.

Furthermore, we used the Arabidopsis system to verify the function of *ZmEREB57* in response to salt stress. Three Arabidopsis *ZmEREB57* overexpression lines (At-OE1, At-OE2 and At-OE3) and one mutant line (*atora47*, *ZmEREB57* homolog in Arabidopsis) were analyzed under salt stress. No phenotypic differences were observed between the transgenic and WT Arabidopsis plants grown on the soil medium under control conditions (Figure S4a). However, after treatment with 200 mM NaCl, WT plants and *atora47* mutants exhibited more severely wilted phenotypes, whereas At-OE1, At-OE2 and At-OE3 maintained a healthy green appearance, and only slight wilting of leaves was observed (Figure S4a). Correspondingly, the fresh weight and chlorophyll content of the overexpression lines under salt stress were significantly higher than those of the WT and *atora47* mutants (Figure S4b,c). Because ZmEREB57 exhibited high conservation of the AP2/ERF domain compared with AtORA47 (Figure S1), we verified whether *ZmEREB57* could complement the *atora47* mutant phenotype by transforming this mutant with the full-length *ZmEREB57* to obtain a restorer line (*atora47*$^{Com\text{-}ZmEREB57}$). In this line, the mutant phenotype was partly complemented, as shown by increased fresh weight and chlorophyll contents under salt stress conditions (Figure S4b,c). These data implied that *ZmEREB57* overexpression enhances tolerance to salinity stress.

3.5 | Identification of ZmEREB57 target genes in maize

DAP-Seq was performed to investigate the target genes regulated by ZmEREB57. This analysis revealed 606 genes that are potentially

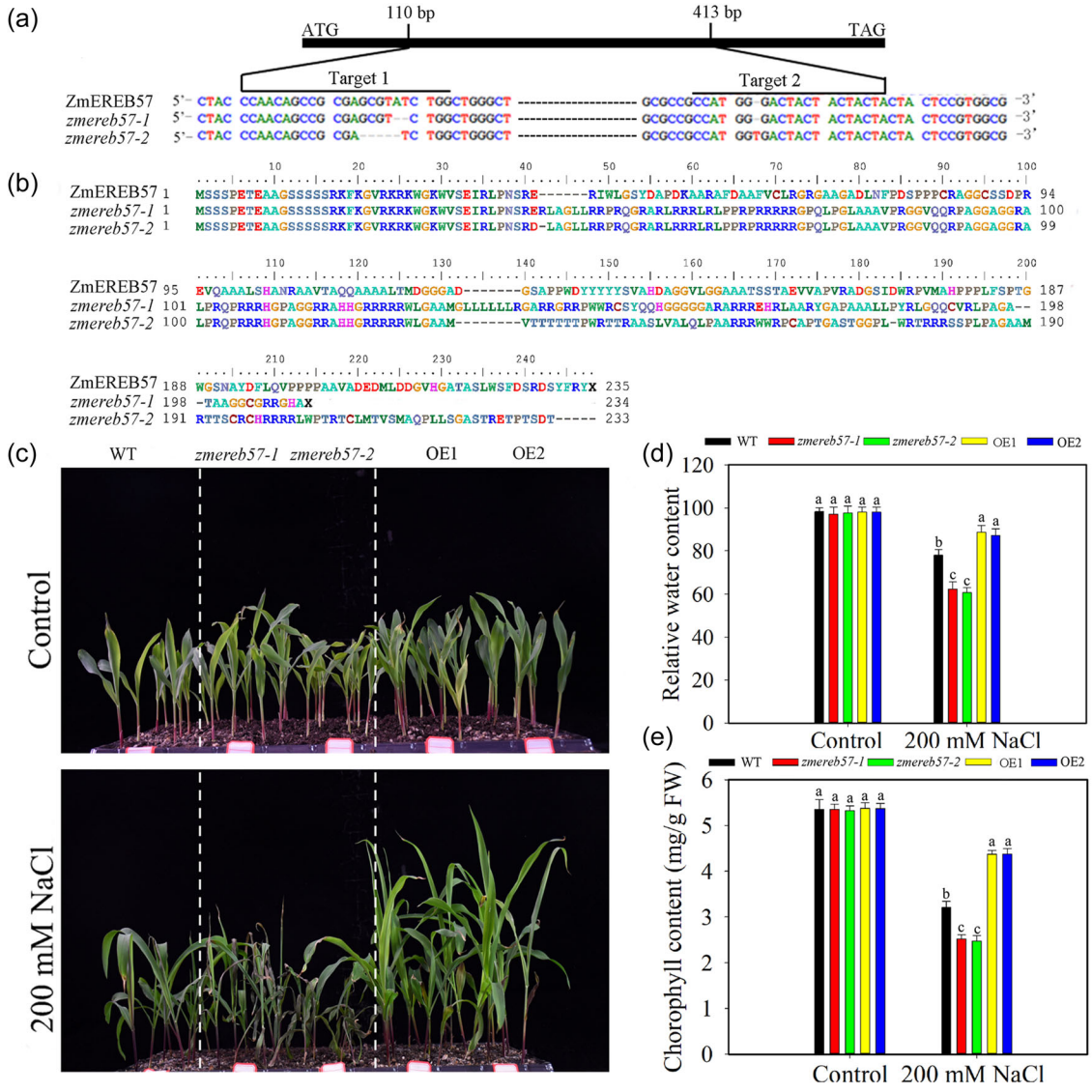

FIGURE 2 Salt tolerance phenotype characterisation in WT, *ZmEREB57* mutated lines (*zmereb57*), and *ZmEREB57* overexpression lines. (a) Targeted mutagenesis of *ZmEREB57* via CRISPR-Cas9. Mutations in two independent lines (*zmereb57*−1 and *zmereb57*−2) are observed, following Sanger sequencing. (b) Alignment of the resulting amino acid sequences of ZmEREB57, *zmereb57*−1 and *zmereb57*−2. Only the sequences flanking the mutations are shown. (c) Appearance of 2-week-old WT, *zmereb57*, and OE plants grown in control and saline soil conditions (supplemented with 200 mM NaCl for 8 days). The relative water content (d) and chlorophyll content (e) were determined in WT, *zmereb57* mutants, and *ZmEREB57* overexpression lines following the salt treatments. Results are expressed as the mean ± *SD* ($n = 3$ replicates). Different letters indicate values which departed significantly from those of WT maize. WT, wild type; ZmEREB57, *Zea mays* Ethylene Responsive Element Binding Factor 57. [Color figure can be viewed at wileyonlinelibrary.com]

targeted by ZmEREB57, with functional annotations across the entire maize genome (Figure 3a). Of the 606 genes, approximately 18% (112) of the ZmEREB57 binding sites were located within the promoter region (2 kb upstream of the TSS) (Figure 3b and Table S3). A specific core binding motif CCGNCC with $p < 0.05$ for ZmEREB57-binding was also revealed (Figure 3c), belonging to the 'O-box like' sequence. The 112 genes with promoter binding sites encoded 7 transcription factors, 9 stress responders, 28 enzymes involved in biological processes, 47 proteins involved in cellular components, and 21 uncharacterised proteins (Figure 3d). These results suggested that ZmEREB57 is a transcription factor with multiple regulatory responses.

3.6 | ZmEREB57 activates *ZmAOC2* expression by directly binding to its promoter

Among the promoter sites bound by ZmEREB57, we found a gene that encodes the allene oxide cyclase2 protein (*Zm00001d053722*, *ZmAOC2*). This gene showed strongly enriched peaks in DAP-seq analysis (Table S3). Further, its wheat homolog, *TaAOC1*, has been reported to be involved in salinity tolerance via JA signalling in wheat (Zhao et al., 2014). The interaction was further studied by screening putative ZmEREB57-binding elements in the promoter of *ZmAOC2* using the Y1H assay. The results revealed that ZmEREB57 specifically

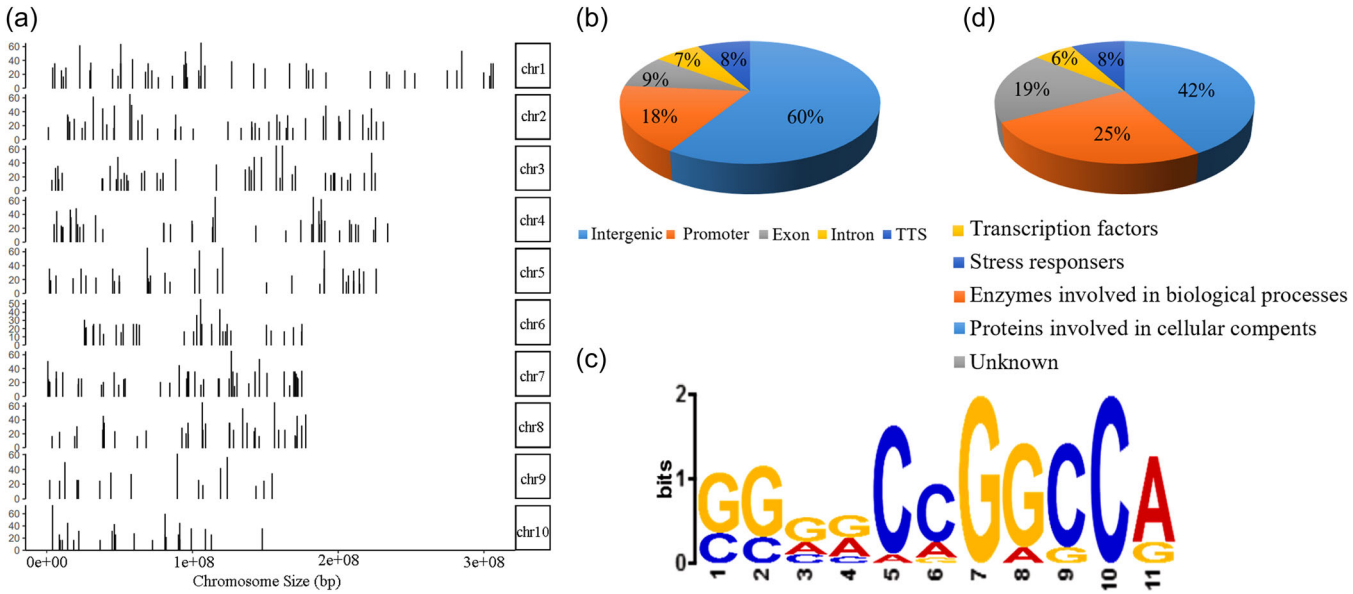

FIGURE 3 DAP-seq (DNA affinity purification sequencing) analysis of ZmEREB57 target genes. (a) Distribution of ZmEREB57-binding sites along the 10 chromosomes of maize. (b) Distribution of ZmEREB57-binding sites in genic and intergenic regions. (c) Motif analysis of combined peaks of ZmEREB57 with the most significant *E*-value. (d) Biological process categorisation of ZmEREB57-regulated target genes. [Color figure can be viewed at wileyonlinelibrary.com]

binds to an 'O-box' like sequence CCGGCC in the promoter region of *ZmAOC2* in yeast (Figure 4a), suggesting that *ZmAOC2* is a potential target gene of ZmEREB57. Luciferase and EMSA assays were performed to confirm the direct binding of ZmEREB57 to the *ZmAOC2* promoter. The first assay showed that ZmEREB57 induced luciferase expression in the presence of the *ZmAOC2* promoter (Figure 4b). For EMSA, a 40-bp oligonucleotide containing the CCGGCC sequence was synthesised based on the sequence of the *ZmAOC2* promoter and labelled as a probe. When the ZmEREB57 protein was incubated with the labelled probe, the migration speed of the protein-DNA complex was reduced (Figure 4c). Competition experiments were performed to determine the specificity of the mobility shift. When the ratio of the unlabelled probe to the labelled probe was 25:1 or 50:1, most labelled probes were weakened (Figure 4c), indicating that the ZmEREB57 protein could bind specifically to the O-box-like region in the *ZmAOC2* promoter. Under control conditions, *ZmAOC2* was expressed at higher levels in the WT and OE maize lines than in both *zmereb57* mutants (Figure 4d). Following salt treatment, *ZmAOC2* expression was further enhanced in the OE lines, followed by the WT plants, whereas very little change was observed in the *zmereb57* mutants (Figure 4d). As expected, the luciferase assay and EMSA results revealed that ZmEREB57 could also bind to the *AtAOC2* promoter in vitro (Figure S5a,b). Similarly, *ZmEREB57* overexpression in Arabidopsis enhanced *AtAOC2* expression under salt-stress conditions (Figure S5c). Collectively, these data indicate that ZmEREB57 binds directly to the *ZmAOC2* promoter and acts as a transcriptional activator.

3.7 | ZmEREB57 affects the accumulation of endogenous OPDA and JA in maize

AOC is a dimeric enzyme localised in chloroplasts, catalysing the formation of OPDA from 13-hydroperoxide linolenic acid, which is then converted into JA in the peroxisomes (Wu et al., 2011; Ziegler et al., 2000). Our analysis of the ZmAOC2-GFP fusion protein suggests that the maize enzyme is also located in chloroplasts (Figure 5a). One *zmaoc2* mutant harbouring a Mu insert (the insertion sites within the first intron of the gene [Figure S6]) was selected to analyze the OPDA and JA content under control and salt stress conditions. In the absence of salt stress, the OPDA and JA contents in the *zmaoc2* mutant were lower than those in the WT plants (B73 lines) (Figure 5b). Treatment with 200 mM NaCl led to an even larger difference in OPDA and JA contents between *zmaoc2* mutant and WT plants, owing to a notable increase in these compounds in the WT plants (Figure 5b). These findings indicate that *ZmAOC2* is involved in OPDA and JA synthesis in maize. Endogenous OPDA and JA levels were also quantified in lines with altered *ZmEREB57* expression. Contents of both compounds were higher in the WT and OE maize lines than in *zmereb57* mutants under control conditions (Figure 5c). Under salt stress, the OE lines had the highest increase in OPDA and JA contents, followed by the WT plants, whereas both *zmereb57* mutants showed more limited increases (Figure 5c). These results suggest that ZmEREB57 affects endogenous OPDA and JA accumulation by regulating *ZmAOC2* expression under salt stress conditions.

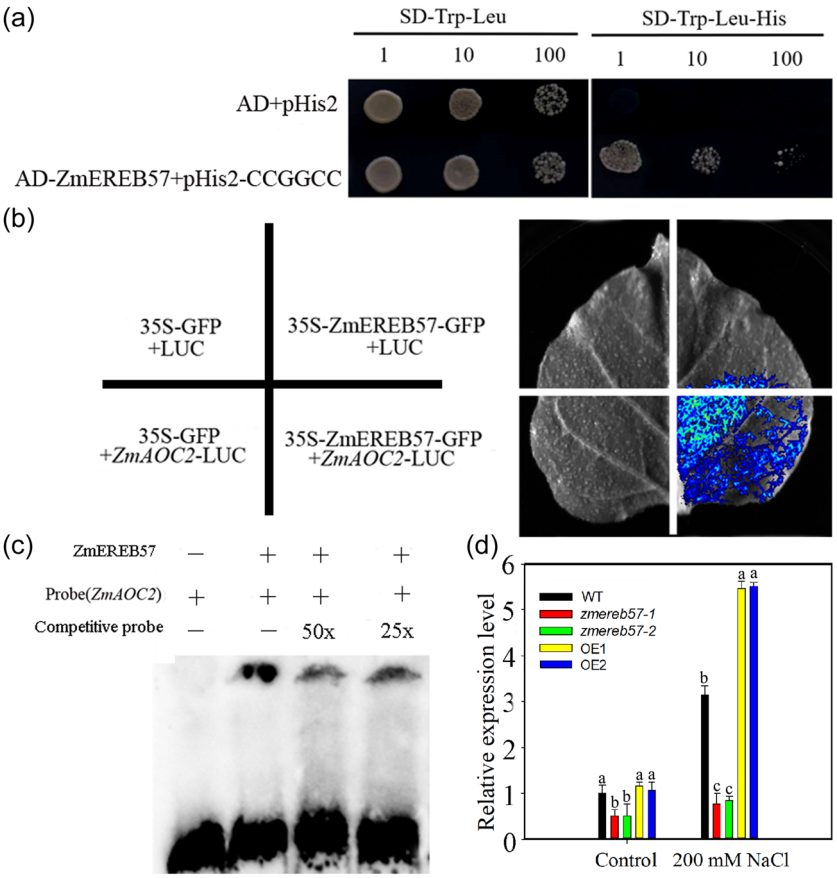

FIGURE 4 ZmEREB57 binds directly to the *ZmAOC2* promoter and activates its expression. (a) The binding activity of ZmEREB57 to the O-box sequence motif, as assessed using a yeast one-hybrid assay. Yeast cells were selected on SD/-Trp/-Leu and SD/-Trp/-Leu/-His media. (b) Luciferase assay for the *ZmAOC2* promoter. The pro*ZmAOC2*:LUC-35S:REN reporter construct was transiently expressed in tobacco leaves together with the control vector or the effector, and images of luciferase signal detection were captured. (c) An electrophoretic mobility shift assay indicates that ZmEREB57 binds to the *ZmAOC2* promoter in vitro. His-ZmEREB57 protein (2 μg) was incubated with labelled probe. Unlabelled (competitive) probe at 25x and 50x molar excess competed with the labelled probe. (d) Relative expression levels of *ZmAOC2* in WT, *zmereb57* mutants, and *ZmEREB57* overexpression lines with and without salt treatment. Different letters indicate values which departed significantly from those of WT maize. AOC2, allene oxide cyclase 2; WT, wild type; ZmEREB57, *Zea mays* Ethylene Responsive Element Binding Factor 57. [Color figure can be viewed at wileyonlinelibrary.com]

3.8 | Exogenous OPDA or JA restores the salt-sensitive phenotype of *zmereb57* mutants

To explore the effect of OPDA and JA on sensitivity to salt stress, we applied exogenous OPDA or JA to the WT, *zmereb57* mutant, and OE lines treated with 200 mM NaCl. Under treatment with 200 mM NaCl without the addition of OPDA or JA, both *zmereb57* mutants exhibited severe wilting and higher water and chlorophyll losses than WT plants (Figure 6a). However, there was no significant phenotypic difference between *zmereb57* mutant lines and WT treated with 100 μm OPDA or 100 μm JA under salt stress (Figure 6a), and the RWC and chlorophyll contents were higher than those with only NaCl treatment (Figure 6b,c). Compared with the control, NaCl stress triggered a significant increase in endogenous OPDA and JA content in WT plants but did not significantly affect endogenous OPDA and JA content in *zmereb57* mutant plants (Figure 6d,e). When plants were treated with OPDA and JA, endogenous OPDA and JA levels increased in the WT and both *zmereb57* mutant plants (Figure 6d,e). Notably, endogenous OPDA and JA levels increased equally in all materials treated with exogenous OPDA, but endogenous OPDA levels increased only slightly in plants treated with exogenous JA (Figure 6d,e). In addition, compared to the WT, both maize OE lines displayed higher RWC, chlorophyll contents, and endogenous OPDA and JA contents under salt stress alone or salt stress with OPDA or JA supplementation (Figure S7). These results indicate that exogenous OPDA or JA application could help restore the salt-tolerant phenotype of *zmereb57* mutants by increasing endogenous OPDA and JA levels.

3.9 | Genes differentially expressed under OPDA and JA treatment participate in salt stress response

To explore the expression patterns of genes regulated by the OPDA/JA pathways in response to salt stress in maize, RNA-seq analyses were conducted on WT plants exposed to salt with or without OPDA or JA treatment. This analysis revealed 6911 DEGs (4089 upregulated and 2822 downregulated) in the NaCl + OPDA treatment and 9454 DEGs (4997 upregulated and 4457 downregulated) in the NaCl + JA treatment compared to the control (Figure 7a, Figure S8a,b, and Table S4–5). Overall, 4032 OPDA- and NaCl-specific response genes (O&NRGs, 58.3% of OPDA-related DEGs) and 5614 JA- and NaCl-specific response genes (JRGs, 46.9% of JA-related DEGs) responded to salt stress (Figure 7a and Table S6–7). Of the total number of DEGs, 2681 ORGs, JRGs and NRGs (O&J&NRGs) were common to all three stimuli (Figure 7a). To gain insight into the biological roles of OPDA or JA in response to salt stress, the biological functions of these genes were mined using the KEGG pathways tool (Figure S8c and Table S8). The results show that these common DEGs from different treatment groups were mainly enriched in various biological pathways related to stress, for example, plant hormone signal transduction, linoleic acid metabolism, and the

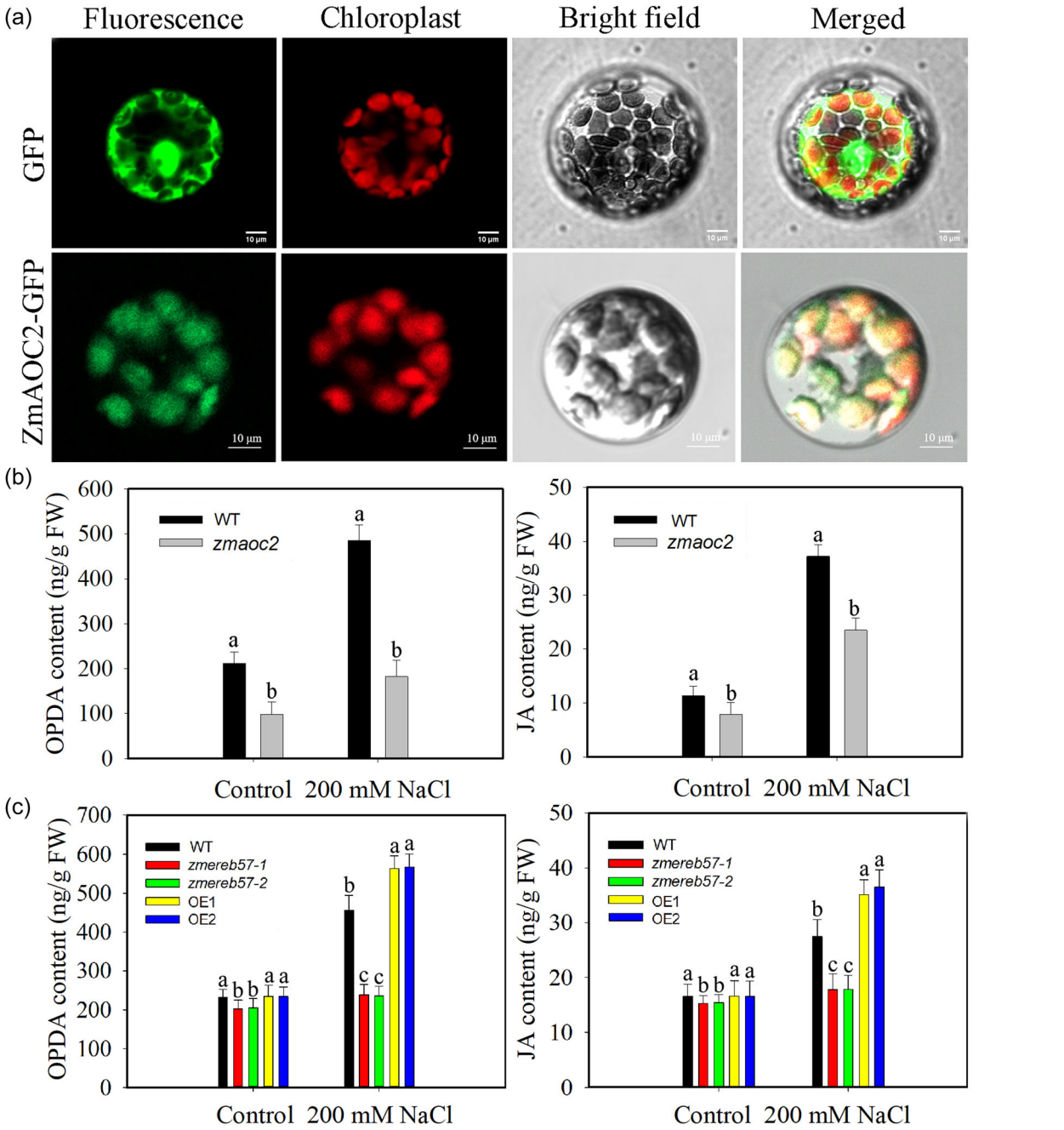

FIGURE 5 Effect of *ZmEREB57* expression on OPDA and JA levels. (a) The subcellular localisation of ZmAOC2-GFP in maize protoplasts cells was visualised using confocal laser scanning microscopy, indicating localisation in the chloroplasts. Scale bar = 10 μm. (b) The levels of OPDA and JA in WT and a *zmaoc2* mutant maize line with or without 200 mM NaCl treatment. (c) The levels of OPDA and JA in WT, *zmereb57* mutants, and *ZmEREB57* overexpression lines with or without 200 mM NaCl treatment. Data are presented as the mean ± *SD* (*n* = 3 replicates). Different letters indicate values which departed significantly from those of WT maize. FW, fresh weight; GFP, green fluorescent protein; JA, jasmonate; OPDA, 12-oxo-phytodienoic acid; WT, wild type; ZmEREB57, *Zea mays* Ethylene Responsive Element Binding Factor 57. [Color figure can be viewed at wileyonlinelibrary.com]

MAPK signalling pathway (Figure S8c). In addition, compared to NaCl alone, JA or OPDA treatment significantly upregulated the expression of genes that encoded TFs or that are involved in phytohormone pathways and redox homeostasis and signalling (Figure 7b). GO enrichment analysis for the upregulated genes in 2681 O&J&NRGs shown that these genes were mostly involved in response to ABA, JA, salt stress, oxidative stress, osmotic stress, and transcription regulation (Figure 7c). These findings suggest that a considerable proportion of the maize transcriptome changes triggered by OPDA and/or JA treatments are involved in the response of plants to salt stress.

To confirm the role of genes involved in the physiological and biochemical processes mediated by OPDA or JA, four O&J&NRGs

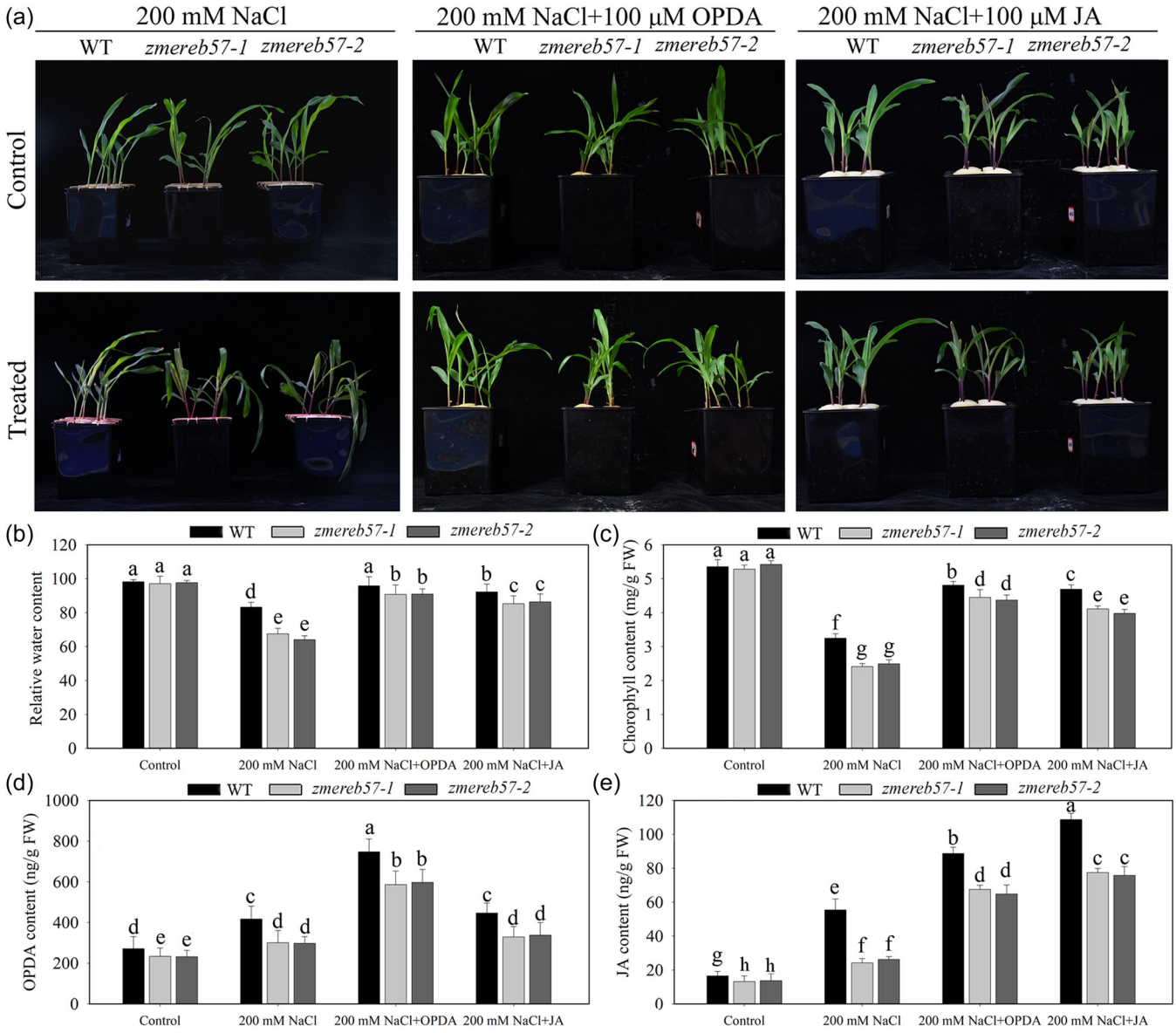

FIGURE 6 Effect of exogenous OPDA or JA on the sensitivity of *zmereb57* mutant plants to salt stress. (a) Appearance of WT and *zmereb57* mutant maize plants grown in high salt conditions and supplemented with 100 μM OPDA or 100 μM JA. Measurements of relative water content (b), chlorophyll (c), OPDA (d), and JA (e) levels were conducted for WT and *zmereb57* mutant plants grown in high salt conditions and supplemented with 100 μM OPDA or 100 μM JA. Data are presented as the mean ± *SD* (*n* = 3 replicates). Different letters indicate values which departed significantly from those of WT maize. FW, fresh weight; JA, jasmonate; OPDA, 12-oxo-phytodienoic acid; WT, wild type; ZmEREB57, *Zea mays* Ethylene Responsive Element Binding Factor 57. [Color figure can be viewed at wileyonlinelibrary.com]

associated with salt stress response processes were selected for RT-PCR analysis in maize WT and *zmereb57* mutants with or without OPDA or JA treatment under salt stress. Our results showed that the expression levels of *WRKY74* (*Zm00001eb310260*), *ABA1* (*Zm00001eb251960*), *MYC2* (*Zm00001eb390330*), and *AP2/ERF134* (*Zm00001eb153470*) were lower in the NaCl-treated plants. In contrast, significantly higher expression levels of *WRKY74*, *ABA1*, *MYC2* and *AP2/ERF134* were observed in OPDA- and JA-treated plants under salt stress (Figure S8d–g). Furthermore, when compared with control plants, NaCl stress triggered a significant increase in ABA content and a decrease in SOD activity; however, these effects were enhanced in OPDA- or JA-treated plants under salt stress (Figure S8h,i).

3.10 | OPDA enhances salinity tolerance through JA-dependent and -independent pathways

Remarkably, there were 1351 O&NRGs that respond specifically to OPDA and NaCl but not to JAs and 2933 J&NRGs that respond specifically to JA and NaCl but not to OPDA (Figure 7a). Further, KEGG enrichment analysis for 1351 O&NRGs and 2933 J&NRGs

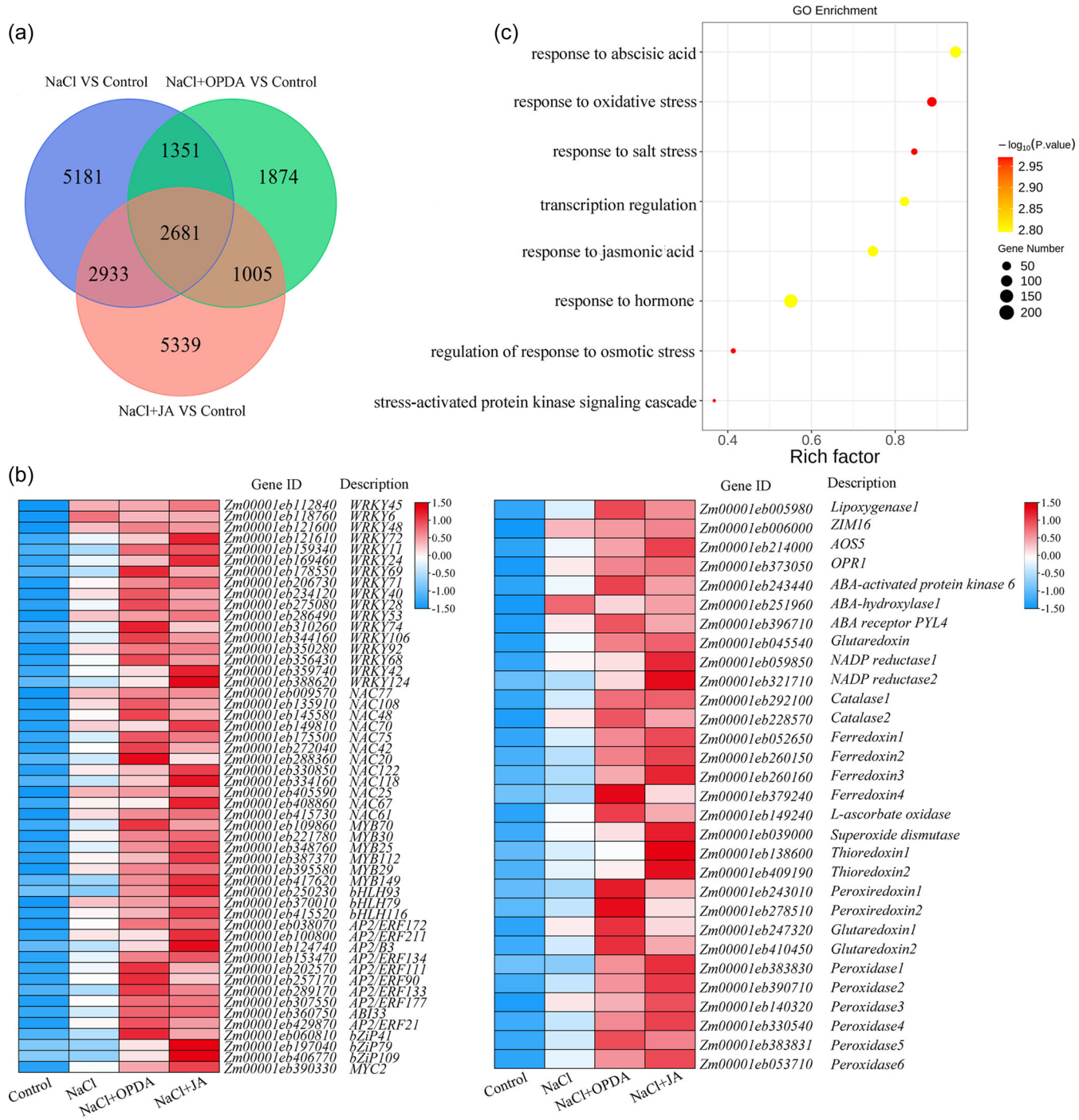

FIGURE 7 Global transcriptome response of maize to salt and phytohormone treatments. (a) Venn diagrams showing the overlap of DEGs identified from the different treatment conditions. (b) Effects of exogenous OPDA or JA on the expression of DEGs related to transcription factors, phytohormone pathways and redox homeostasis in maize seedlings under salt stress. (c) GO enrichment annotation for the upregulated genes in 2681 DEGs shared between treatments with 200 mM NaCl alone, 200 mM NaCl supplemented with 100 μM OPDA, and the 200 mM NaCl supplemented with 100 μM JA treatment. Numbers next to each bar represent the number of DEGs. DEG, differentially expressed gene; GO, gene ontology; JA, jasmonate; OPDA, 12-oxo-phytodienoic acid. [Color figure can be viewed at wileyonlinelibrary.com]

revealed that these genes were related to various abiotic stress responses, such as plant hormone signal transduction and the MAPK signalling pathway (Figure S9a,b). These results indicated that OPDA confers tolerance to salt stress independently as well as cooperatively with JA. To verify this hypothesis, we utilised two maize JA biosynthesis mutants: *aoc2*, which cannot synthesise either OPDA or JA and *opr3* (*Zm00001d032049*, the insertion sites within the first exon of the gene [Figure S6]), which contains a defect in JA biosynthesis. Both *zmaoc2* and *zmopr3* mutants exhibited more severe wilting and higher water and chlorophyll loss than the WT

under the 200 mM NaCl treatment (Figure 8a–c). Furthermore, when supplemented with 100 μM OPDA under salt treatment, *zmaoc2*, *zmopr3* mutants, and the WT showed similar phenotypic characteristics (Figure 8a–c). In contrast, when supplemented with 100 μM JA under salt treatment, only the *zmopr3* mutant exhibited a similar appearance to the WT, whereas the *zmaoc2* mutant appeared more sensitive than the *zmopr3* mutant and WT (Figure 8a–c).

To determine whether OPDA is required to induce the expression of ORGs in vivo under salt stress, we assessed the expression profile of three putative O&NRGs genes, including *ZAT10* (*Zm00001eb064620*), *ERF9* (*Zm00001eb369560*), and *DREB1* (*Zm00001eb073550*), and one J&NRGs gene *VSP9a* (*Zm00001eb398120*) in the *zmaoc2* and *zmopr3* mutants (Figure S9c–f). No significant differences were observed in the expression levels of the four genes between the mutants and WT plants under control conditions. The transcription levels of all four genes were lower in the *zmaoc2* mutant plants compared with those in the WT plants under salt treatment (Figure S9c–f). Under salt stress, treatment with OPDA, but not JA, increased the expression of *ZAT10*, *ERF9* and *DREB1* in the WT, *zmaoc2* mutants, and *zmopr3* mutants (Figure S9c,e). While *VSP9a* was clearly upregulated by OPDA and JA treatment in the WT and *zmaoc2* mutant plants under salt stress, it was only slightly induced in the *opr3* mutant by OPDA treatment (Figure S9f).

4 | DISCUSSION

In maize, AP2/ERF has emerged as an extensive transcription factor family with 292 potential members (Du et al., 2014), and several maize AP2/ERF TFs have been implicated in the adaptive responses of plants to environmental stresses. For example, ZmEREB20 positively responds to salt tolerance by regulating ABA- and ROS scavenging-related genes (Fu et al., 2021), and ZmEREB46 is involved in the drought stress response by influencing the biosynthesis of waxes and cutin (Yang et al., 2022). In the present study, ZmEREB57 was identified as a member of the AP2/ERF family in maize based on phylogenetic and sequence analyses (Figure S1). *ZmEREB57* expression was also markedly induced by salt stress (Figure S2) and loss of function mutations in *ZmEREB57* resulted in the enhanced maize sensitivity to salt stress (Figure 2). Inversely overexpression of

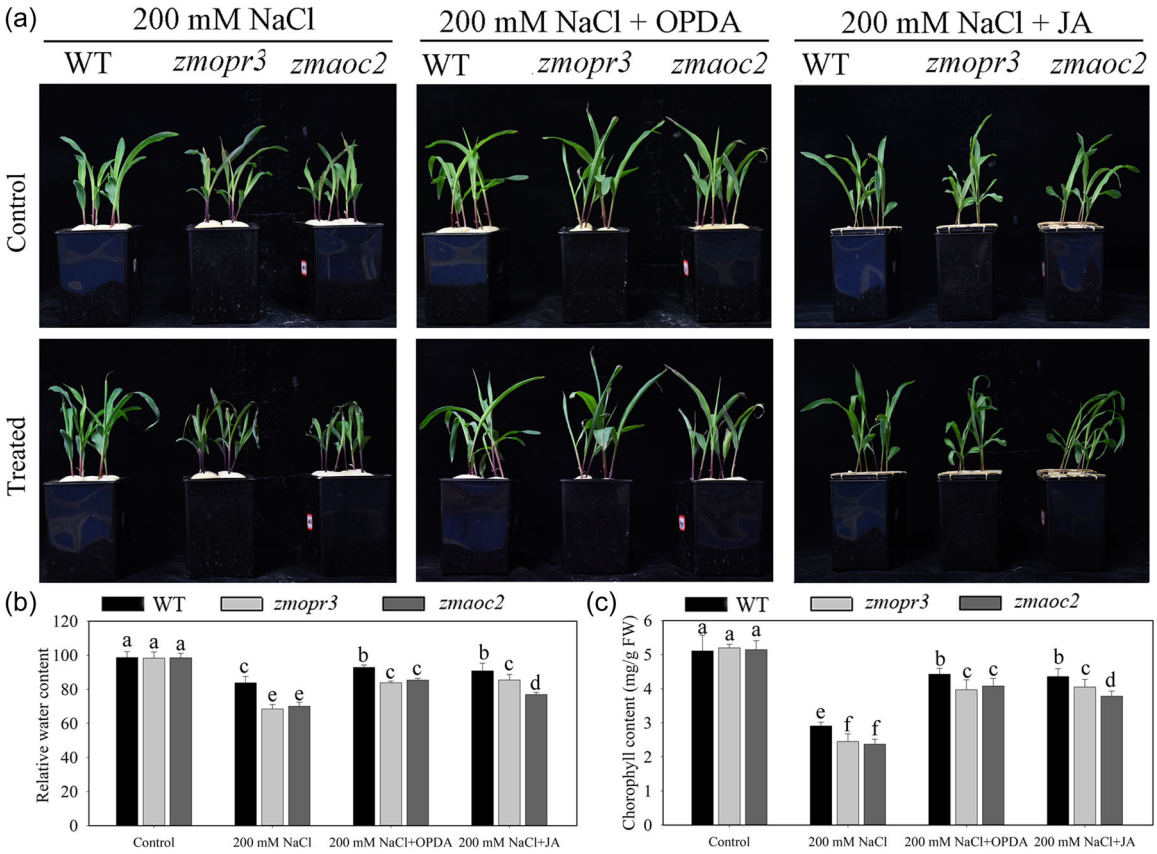

FIGURE 8 Characteristics of OPDA and JA biosynthesis mutants under conditions of salt stress. Phenotype (a), relative water content (b), and chlorophyll levels (c) of maize WT, *zmaoc2* and *zmopr3* mutants before and after treatment with 200 mM NaCl, 200 mM NaCl supplemented with 100 μM OPDA, and 200 mM NaCl supplemented with 100 μM JA. Data are represented as the mean ± *SD* ($n = 3$ replicates). Different letters indicate values which departed significantly from those of WT maize. JA, jasmonate; OPDA, 12-oxo-phytodienoic acid; WT, wild type. [Color figure can be viewed at wileyonlinelibrary.com]

ZmEREB57 in maize or Arabidopsis plants enhanced salt tolerance (Figure 2 and Figure S4). Therefore, we conclude that *ZmEREB57* plays a role in increasing salinity tolerance.

The AP2/ERF TFs activate a series of target genes to mediate stress tolerance by binding to *cis*-acting elements. For example, AtORA47 was shown to bind to the O-box [(NC/GT) CGNCCA] involved in the biosynthesis of JA and ABA (Chen et al., 2016). OsEREBP1 regulates the expression of genes involved in abiotic stress responses containing a GCC box in their promoters (Jisha et al., 2015). DAP-Seq revealed that ZmEREB57 preferentially binds to an O-box-like motif in the promoter of the *ZmAOC2* gene (Figure 4a–c), and ZmEREB57 was observed to promote *ZmAOC2* expression in the OE lines under salt stress conditions (Figure 4d). Overexpression of *AOC* in Arabidopsis and wheat increased JA levels and enhanced tolerance to salt stress, indicating that this enzyme may play a role in certain stress responses by regulating OPDA or JA content (Zhao et al., 2014). We confirmed that ZmAOC2 was localised in chloroplasts, and *zmaoc2* mutants affected OPDA and JA levels under salt stress conditions (Figure 5a,b). Thus, we deduced that ZmEREB57 promotes the accumulation of OPDA and JA by regulating *ZmAOC2* expression in response to salt stress in maize.

JAs are important in the regulation of plant responses to environmental stress (Jung et al., 2007). The COI-JAZ-MYC complex is considered a central component of signalling pathways involving JAs, and at least a subfraction of COI1-dependent genes is induced following tissue damage as well as under various types of abiotic stresses, including salt treatment (Geng et al., 2013), osmotic stress (Grebner et al., 2013), and drought (Huang et al., 2008). OPDA, a precursor of JA, also induces the expression of certain genes in response to several stresses (Ribot et al., 2008). A total of 2,681 DEGs were differentially expressed under salt stress, as well as by OPDA and JA treatment, and many of these genes are annotated to be involved in transcriptional regulation, phytohormone functions, and antioxidant systems. The expression of such genes was notably increased significantly by OPDA or JA treatment (Figure 6 and Figure S8), suggesting that OPDA or JA and its associated response genes are required for coping with saline conditions. For example, many TFs, such as those belonging to the bZIP, MYB, NAC and WRKY families, may activate or inhibit factors that participate in salt stress responses (Abe et al., 2003; Hu et al., 2008; Jakoby et al., 2002; Ma et al., 2019; Wei et al., 2017). ABA accumulation can accelerate stomatal closure and upregulate the expression of stress-responsive genes, resulting in increased salt stress tolerance in plants (Wu et al., 2009). In addition, the antioxidative defence system, consisting of ROS scavenging and redox-related enzymes, can alleviate oxidative damage induced by salt stress (Chardin et al., 2017).

JA and OPDA have individual signalling properties and differ in gene expression patterns. Transcriptomic analyses have revealed distinct sets of genes that are regulated specifically by OPDA, but not JA (Stintzi et al., 2001), and proteomic analysis of approximately 6000 proteins in *A. thaliana* showed that approximately 5% of wound-inducible proteins are synthesised independently of JA (Gfeller et al., 2011). We used RNA-seq analysis to identify the genes that responded to OPDA or JA treatment (Figure 7 and Figure S8).

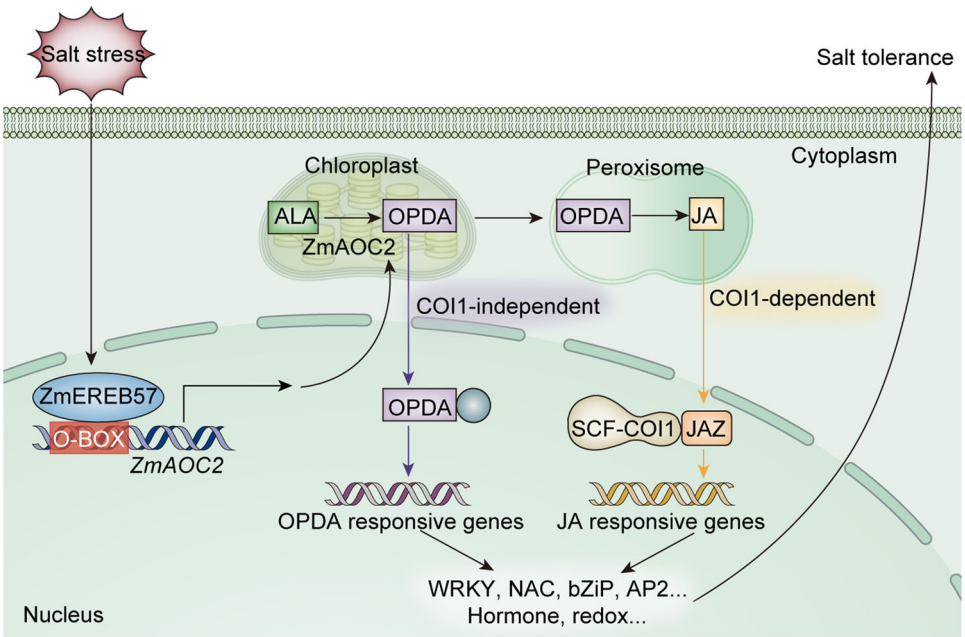

FIGURE 9 A proposed model describing the regulatory role of *ZmEREB57* in response to salt stress. Salt stress induces the expression of *ZmEREB57*, and ZmEREB57 activates the transcription of *ZmAOC2* by directly binding to O-box element in the promoter. The induction of *ZmAOC2* leads to increased OPDA and JA accumulation, directly or indirectly. Either directly via a COI1-independent route or indirectly through the JA-COI1-dependent pathway, OPDA regulate the expression of stress-related genes, thereby conferring increased tolerance to salt stress in *Z. mays*. OPDA, 12-oxo-phytodienoic acid. [Color figure can be viewed at wileyonlinelibrary.com]

The DEGs shared between JA and OPDA stimulation included signalling components, genes involved in metabolic pathways, and TFs, whereas the characteristics of J&NRGs and O&NRG differed significantly (Figure 7 and Figure S8). Saline treatment increased the expression of OPDA-specific response genes in *zmopr3* mutants but not *zmaoc2* mutants, whereas the addition of exogenous OPDA induced their expression in the *zmaoc2* mutants (Figure S9c). We found that the expression of *ZmVSP9a*, a homolog of *AtVSP2*, was lower in both mutants that could not accumulate JA than in the WT plants under salt stress conditions (Figure S9c). Treatment with exogenous JA, but not OPDA, restored the expression of *ZmVSP9a* to that observed in the WT in the *zmopr3* but not the *zmaoc2* line (Figure S9c). These findings suggest that OPDA functions as a signalling mediator in the maize salt response through a mechanism distinct from that of JAs.

Based on these results, a functional model of ZmEREB57 response to salt stress is proposed (Figure 9). ZmEREB57 is a transcription factor that binds to the *cis*-acting motifs O-box in the promoter to regulate the transcription of genes such as *ZmAOC2*. Induction of *ZmAOC2* significantly increases the biosynthesis of OPDA and JA. OPDA and JA orchestrate the regulatory network of salt-responsive genes in a COI-independent and COI1-dependent manner, respectively, thereby conferring increased tolerance to salt stress in *Z. mays*. We conclude that *ZmEREB57* is an important genetic resource that can enhance salt tolerance in maize, Arabidopsis, and perhaps other plants, owing to its upregulation in response to salt.

ACKNOWLEDGEMENTS

We thank Fanguo Chen (Shandong University) for reviewing the manuscript and providing excellent suggestions for improvement. We thank the ChinaMu Project for providing maize mutants. This research was supported by grants from the National Natural Science Foundation of China (31901497 and 32272075), the National Key Research and Development Program of China (2022YFD1201502), and Science and Technology Program of University of Jinan (XKY2207).

CONFLICT OF INTEREST STATEMENT

The authors declare no conflicts of interest.

ORCID

Jiantang Zhu http://orcid.org/0000-0002-4706-586X
Hui Li http://orcid.org/0000-0002-9021-8091

REFERENCES

Abbaraju, H.K.R., Gupta, R., Appenzeller, L.M., Fallis, L.P., Hazebroek, J., Zhu, G. et al. (2022) A vegetative storage protein improves drought tolerance in maize. *Plant Biotechnology Journal*, 20, 374–389.

Abe, H., Urao, T., Ito, T., Seki, M., Shinozaki, K. & Yamaguchi-Shinozaki, K. (2003) Arabidopsis AtMYC2 (bHLH) and AtMYB2 (MYB) function as transcriptional activators in abscisic acid signaling. *The Plant Cell*, 15, 63–78.

Acosta, F., Laparra, H., Romero, S.P., Schmelz, E., Hamberg, M., Mottinger, J.P. et al. (2009) Tasselseed1 is a lipoxygenase affecting jasmonic acid signaling in sex determination of maize. *Science*, 323, 262–265.

Anders, S. & Huber, W. (2010) Differential expression analysis for sequence count data. *Genome Biology*, 11, R106.

Bartels, D. & Sunkar, R. (2005) Drought and salt tolerance in plants. *Critical Reviews in Plant Sciences*, 24, 23–58.

Bartlett, A., O'Malley, R.C., Huang, S.C., Galli, M., Nery, J.R., Gallavotti, A. et al. (2017) Mapping genome-wide transcription-factor binding sites using DAP-seq. *Nature Protocols*, 12, 1659–1672.

Borkiewicz, L., Polkowska-Kowalczyk, L., Cieśla, J., Sowiński, P., Jończyk, M., Rymaszewski, W. et al. (2020) Expression of maize calcium-dependent protein kinase (ZmCPK11) improves salt tolerance in transgenic Arabidopsis plants by regulating sodium and potassium homeostasis and stabilizing photosystem II. *Physiologia Plantarum*, 168, 38–57.

Cao, J., Yao, D., Lin, F. & Jiang, M. (2014) PEG-mediated transient gene expression and silencing system in maize mesophyll protoplasts: a valuable tool for signal transduction study in maize. *Acta Physiologiae Plantarum*, 36, 1271–1281.

Chardin, C., Schenk, S.T., Hirt, H., Colcombet, J. & Krapp, A. (2017) Review: mitogen-activated protein kinases in nutritional signaling in Arabidopsis. *Plant Science*, 260, 101–108.

Chen, H.Y., Hsieh, E.J., Cheng, M.C., Chen, C.Y., Hwang, S.Y. & Lin, T.P. (2016) ORA47 (octadecanoid-responsive AP2/ERF-domain transcription factor 47) regulates jasmonic acid and abscisic acid biosynthesis and signaling through binding to a novel cis-element. *New Phytologist*, 211, 599–613.

Chini, A., Monte, I., Zamarreño, A.M., Hamberg, M., Lassueur, S., Reymond, P. et al. (2018) An OPR3-independent pathway uses 4,5-didehydrojasmonate for jasmonate synthesis. *Nature Chemical Biology*, 14, 171–178.

Clough, S.J. & Bent, A.F. (1998) Floral dip: a simplified method for agrobacterium-mediated transformation of *Arabidopsis thaliana*. *The Plant Journal*, 16, 735–743.

Dave, A. & Graham, I.A. (2012) Oxylipin signaling: a distinct role for the jasmonic acid precursor cis-(+)−12-Oxo-phytodienoic acid (cis-OPDA). *Frontiers in Plant Science*, 3, 42.

Dave, A., Hernández, M.L., He, Z., Andriotis, V.M.E., Vaistij, F.E., Larson, T.R. et al. (2011) 12-Oxo-phytodienoic acid accumulation during seed development represses seed germination in Arabidopsis. *The Plant Cell*, 23, 583–599.

Fu, J.Y., Zhu, C.Y., Wang, C., Liu, L.J., Shen, Q.Q., Xu, D.B. et al. (2021) Maize transcription factor ZmEREB20 enhanced salt tolerance in transgenic Arabidopsis. *Plant Physiology and Biochemistry*, 159, 257–267.

Geng, Y., Wu, R., Wee, C.W., Xie, F., Wei, X., Chan, P.M.Y. et al. (2013) A spatio-temporal understanding of growth regulation during the salt stress response in Arabidopsis. *The Plant Cell*, 25, 2132–2154.

Gfeller, A., Baerenfaller, K., Loscos, J., Chételat, A., Baginsky, S. & Farmer, E.E. (2011) Jasmonate controls polypeptide patterning in undamaged tissue in wounded Arabidopsis leaves. *Plant Physiology*, 156, 1797–807.

Grebner, W., Stingl, N.E., Oenel, A., Mueller, M.J. & Berger, S. (2013) Lipoxygenase6-dependent oxylipin synthesis in roots is required for abiotic and biotic stress resistance of Arabidopsis. *Plant Physiology*, 161, 2159–2170.

Hao, L., Shi, S., Guo, H., Li, M., Hu, P., Wei, Y. et al. (2020) Genome-wide identification and expression profiles of ERF subfamily transcription factors in *Zea mays*. *PeerJ*, 8, e9551.

Hu, H., You, J., Fang, Y., Zhu, X., Qi, Z. & Xiong, L. (2008) Characterization of transcription factor gene SNAC2 conferring cold and salt tolerance in rice. *Plant Molecular Biology*, 67, 169–181.

Huang, D., Wu, W., Abrams, S.R. & Cutler, A.J. (2008) The relationship of drought-related gene expression in *Arabidopsis thaliana* to hormonal and environmental factors. *Journal of Experimental Botany*, 59, 2991–3007.

Jakoby, M., Weisshaar, B., Dröge-Laser, W., Vicente-Carbajosa, J., Tiedemann, J., Kroj, T. et al. (2002) bZIP transcription factors in Arabidopsis. *Trends in Plant Science*, 7, 106–111.

Jia, H., Li, M., Li, W., Liu, L., Jian, Y., Yang, Z. et al. (2020) A serine/threonine protein kinase encoding gene KERNEL NUMBER PER ROW6 regulates maize grain yield. *Nature Communications*, 11, 988.

Jisha, V., Dampanaboina, L., Vadassery, J., Mithöfer, A., Kappara, S. & Ramanan, R. (2015) Overexpression ofan AP2/ERF type transcription factor OsEREBP1 confers biotic and abiotic stress tolerance in rice. *PLoS One*, 10, e0127831.

Jung, C., Lyou, S.H., Yeu, S., Kim, M.A., Rhee, S., Kim, M. et al. (2007) Microarray-based screening of jasmonate-responsive genes in *Arabidopsis thaliana*. *Plant Cell Reports*, 26, 1053–1063.

Kang, D.J., Seo, Y.J., Lee, J.D., Ishii, R., Kim, K.U., Shin, D.H. et al. (2005) Jasmonic acid differentially affects growth, ion uptake and abscisic acid concentration in salt-tolerant and salt-sensitive rice cultivars. *Journal of Agronomy and Crop Science*, 191, 273–282.

Kienow, L., Schneider, K., Bartsch, M., Stuible, H.P., Weng, H., Miersch, O. et al. (2008) Jasmonates meet fatty acids: functional analysis of a new acyl-coenzyme A synthetase family from *Arabidopsis thaliana*. *Journal of Experimental Botany*, 59, 403–419.

Langmead, B. & Salzberg, S.L. (2012) Fast gapped-read alignment with Bowtie 2. *Nature Methods*, 9, 357–359.

Liang, L., Zhou, L., Tang, Y., Li, N., Song, T., Shao, W. et al. (2019) A sequence-indexed mutator insertional library for maize functional genomics study. *Plant Physiology*, 181, 1404–1414.

Lin, R., Zhao, W., Meng, X. & Peng, Y.L. (2007) Molecular cloning and characterization of a rice gene encoding AP2/EREBP-type transcription factor and its expression in response to infection with blast fungus and abiotic stresses. *Physiological and Molecular Plant Pathology*, 70, 60–68.

Ma, Q., Xia, Z., Cai, Z., Li, L., Cheng, Y., Liu, J. et al. (2019) GmWRKY16 enhances drought and salt tolerance through an ABA-mediated pathway in *Arabidopsis thaliana*. *Frontiers in Plant Science*, 9, 1979.

Machanick, P. & Bailey, T.L. (2011) MEME-ChIP: motif analysis of large DNA datasets. *Bioinformatics*, 27, 1696–1697.

Mizoi, J., Shinozaki, K. & Yamaguchi-Shinozaki, K. (2012) AP2/ERF family transcription factors in plant abiotic stress responses. *Biochimica et Biophysica Acta (BBA)-Gene Regulatory Mechanisms*, 1819, 86–96.

Ni, L., Fu, X., Zhang, H., Li, X., Cai, X., Zhang, P. et al. (2019) Abscisic acid inhibits rice protein phosphatase PP_{45} via H_2O_2 and relieves repression of the Ca^{2+}/CaM-dependent protein kinase DMI3. *The Plant Cell*, 31, 128–152.

Qin, F., Kakimoto, M., Sakuma, Y., Maruyama, K., Osakabe, Y., Tran, L.S.P. et al. (2007) Regulation and functional analysis of ZmDREB2A in response to drought and heat stresses in *Zea mays* L. *The Plant Journal*, 50, 54–69.

Ribot, C., Zimmerli, C., Farmer, E.E., Reymond, P. & Poirier, Y. (2008) Induction of the Arabidopsis *PHO1; H10* gene by 12-oxo-phytodienoic acid but not jasmonic acid via a *CORONATINE INSENSITIVE1*-dependent pathway. *Plant Physiology*, 147, 696–706.

Sakuma, Y., Liu, Q., Dubouzet, J.G., Abe, H., Shinozaki, K. & Yamaguchi-Shinozaki, K. (2002) DNA-binding specificity of the ERF/AP2 domain of Arabidopsis DREBs, transcription factors involved in dehydration- and cold-inducible gene expression. *Biochemical and Biophysical Research Communications*, 290, 998–1009.

Satoh, M., Tokaji, Y., Nagano, A.J., Hara-Nishimura, I., Hayashi, M., Nishimura, M. et al. (2014) Arabidopsis mutants affecting oxylipin signaling in photo-oxidative stress responses. *Plant Physiology and Biochemistry*, 81, 90–95.

Savchenko, T. & Dehesh, K. (2014) Drought stress modulates oxylipin signature by eliciting 12-OPDA as a potent regulator of stomatal aperture. *Plant Signaling & Behavior*, 9, e28304.

Savchenko, T., Kolla, V.A., Wang, C.Q., Nasafi, Z., Hicks, D.R., Phadungchob, B. et al. (2014) Functional convergence of oxylipin and abscisic acid pathways controls stomatal closure in response to drought. *Plant Physiology*, 164, 1151–1160.

Staswick, P.E. & Tiryaki, I. (2004) The oxylipin signal jasmonic acid is activated by an enzyme that conjugates it to isoleucine in Arabidopsis. *The Plant Cell*, 16, 2117–2127.

Stintzi, A., Weber, H., Reymond, P., Browse, J. & Farmer, E.E. (2001) Plant defense in the absence of jasmonic acid: the role of cyclopentenones. *Proceedings of the National Academy of Sciences*, 98, 12837–12842.

Stumpe, M., Göbel, C., Faltin, B., Beike, A.K., Hause, B., Himmelsbach, K. et al. (2010) The moss *Physcomitrella patens* contains cyclopentenones but no jasmonates: mutations in allene oxide cyclase lead to reduced fertility and altered sporophyte morphology. *New Phytologist*, 188, 740–749.

Sugano, S., Sugimoto, T., Takatsuji, H. & Jiang, C.J. (2013) Induction of resistance to phytophthora sojaein soyabean (*Glycine Max*) by salicylic acid and ethylene. *Plant Pathology*, 62, 1048–1056.

Takeuchi, K., Gyohda, A., Tominaga, M., Kawakatsu, M., Hatakeyama, A., Ishii, N. et al. (2011) RSOsPR10 expression in response to environmental stresses is regulated antagonistically by jasmonate/ethylene and salicylic acid signaling pathways in rice roots. *Plant and Cell Physiology*, 52, 1686–1696.

Taki, N., Sasaki-Sekimoto, Y., Obayashi, T., Kikuta, A., Kobayashi, K., Ainai, T. et al. (2005) 12-oxo-phytodienoic acid triggers expression of a distinct set of genes and plays a role in wound-induced gene expression in Arabidopsis. *Plant Physiology*, 139, 1268–1283.

Thines, B., Katsir, L., Melotto, M., Niu, Y., Mandaokar, A., Liu, G. et al. (2007) JAZ repressor proteins are targets of the SCF(COI1) complex during jasmonate signalling. *Nature*, 448, 661–665.

Wasternack, C. & Hause, B. (2013) Jasmonates: biosynthesis, perception, signal transduction and action in plant stress response, growth and development. *Annals of Botany*, 111, 1021–1058.

Wasternack, C. & Strnad, M. (2016) Jasmonate signaling in plant stress responses and development-active and inactive compounds. *New Biotechnology*, 33, 604–613.

Wei, Q., Luo, Q., Wang, R., Zhang, F., He, Y., Zhang, Y. et al. (2017) A wheat R2R3-type MYB transcription factor TaODORANT1 positively regulates drought and salt stress responses in transgenic tobacco plants. *Frontiers in Plant Science*, 8, 1374.

Wu, Q., Wu, J., Sun, H., Zhang, D. & Yu, D. (2011) Sequence and expression divergence of the AOC gene family in soybean: insights into functional diversity for stress responses. *Biotechnology Letters*, 33, 1351–1359.

Wu, X., Shiroto, Y., Kishitani, S., Ito, Y. & Toriyama, K. (2009) Enhanced heat and drought tolerance in transgenic rice seedlings overexpressing OsWRKY11 under the control of *HSP101* promoter. *Plant Cell Reports*, 28, 21–30.

Xing, H.L., Dong, L., Wang, Z.P., Zhang, H.Y., Han, C.Y., Liu, B. et al. (2014) A CRISPR/Cas9 toolkit for multiplex genome editing in plants. *BMC Plant Biology*, 14, 327.

Xu, Z.S., Chen, M., Li, L.C. & Ma, Y.Z. (2011) Functions and application of the AP2/ERF transcription factor family in crop improvement. *Journal of Integrative Plant Biology*, 53, 570–585.

Yamamoto, Y., Ohshika, J., Takahashi, T., Ishizaki, K., Kohchi, T., Matusuura, H. et al. (2015) Functional analysis of allene oxide cyclase, MpAOC, in the liverwort *Marchantia polymorpha*. *Phytochemistry*, 116, 48–56.

Young, M.D., Wakefield, M.J., Smyth, G.K. & Oshlack, A. (2010) Gene ontology analysis for RNA-seq: accounting for selection bias. *Genome Biology*, 11, R14.

Yang, Y., Shi, J.X., Chen, L.M., Xiao, W.H. & Yu, J.J. (2022) ZmEREB46, a maize ortholog of Arabidopsis WAX INDUCER1/SHINE1, is involved in the biosynthesis of leaf epicuticular very-long-chain waxes and drought tolerance. *Plant Science*, 321, 111256.

Zhang, F., Ke, J., Zhang, L., Chen, R., Sugimoto, K., Howe, G.A. et al. (2017) Structural insights into alternative splicing-mediated desensitization of jasmonate signaling. *Proceedings of the National Academy of Sciences*, 114, 1720–1725.

Zhang, J., Simmons, C., Yalpani, N., Crane, V., Wilkinson, H. & Kolomiets, M. (2005) Genomic analysis of the 12-oxophytodienoic acid reductase gene family of *Zea mays*. *Plant Molecular Biology*, 59, 323–343.

Zhang, Y., Liu, T., Meyer, C.A., Eeckhoute, J., Johnson, D.S., Bernstein, B.E. et al. (2008) Model-based analysis of ChIP-Seq (MACS). *Genome Biology*, 9, R137.

Zhao, Y., Dong, W., Zhang, N., Ai, X., Wang, M., Huang, Z. et al. (2014) A wheat allene oxide cyclase gene enhances salinity tolerance via jasmonate signaling. *Plant Physiology*, 164, 1068–1076.

Ziegler, J., Stenzel, I., Hause, B., Maucher, H., Hamberg, M., Grimm, R. et al. (2000) Molecular cloning of allene oxide cyclase. *Journal of Biological Chemistry*, 275, 19132–19138.

SUPPORTING INFORMATION

Additional supporting information can be found online in the Supporting Information section at the end of this article.

How to cite this article: Zhu, J., Wei, X., Yin, C., Zhou, H., Yan, J., He, W. et al. (2023) ZmEREB57 regulates OPDA synthesis and enhances salt stress tolerance through two distinct signaling pathways in *Zea mays*. *Plant, Cell & Environment*, 1–17. https://doi.org/10.1111/pce.14644